Pulse Wave Generation Method for PPG by using Display

Atsuhiro Fujii
Ritsumeikan University
Shiga, Japan
atsuhiro.fujii@iis.ise.ritsumei.ac.jp

Kazuya Murao
Ritsumeikan University / Japan Science and Technology Agency, PRESTO
Shiga, Japan
murao@cs.ritsumei.ac.jp

Naoji Matsuhisa
Keio University / Japan Science and Technology Agency, PRESTO
Kanagawa, Japan
naoji@keio.jp

ABSTRACT

The extensive research on wearable devices has led to devices of various shapes and wearing areas. Wearable devices are often used to record the user's biometric information, and methods to detect physical abnormalities from the acquired data have been proposed. Among biometric data, pulse data has been used in methods such as heart rate monitoring and emotion recognition. The most common type of pulse sensor is the photoplethysmogram (PPG), which irradiates a green LED on the skin and measures pulse data from changes in the light reflected through the blood vessels. PPG sensors have been implemented in commercially available wearable devices such as smartwatches. The PPG sensor requires blood flow for data acquisition due to the characteristics of the mechanism. When a smartwatch is worn on an artificial body such as a prosthetic hand or a robotic arm, correct data cannot be acquired because there is no blood flow. In this study, we propose a method that enables the PPG sensor to measure arbitrary pulse data using a display. If this method is successful, it will be possible to input pulse data measured at the junction of the live body and the prosthetic hand to the display, and have the smartwatch attached to the prosthetic hand read the same pulse data. In this paper, we focus on the heart rate and report the results of an experiment in which a target heart rate was input and the display was controlled to determine whether the target heart rate could be obtained by a smartwatch. We implemented a display drawing program and conducted the evaluation using five kinds of smartwatches and four kinds of displays. Results showed that the error between the target heart rate and the heart rate acquired by the smartwatch was within 3 beats per minute in many cases when the target heart rate was set to 60–100. When the target heart rate was set to 40–55 and 105–200, the heart rate could be input to the smartwatch with a small error under some conditions. When the generated PPG data was imported into a heart rate variability (HRV) analysis software, it was recognized as a pulse wave in the same way as real PPG data obtained from a body. We compared the heart rate, SDNN, RR interval, and LF/HF ratio calculated from the real PPG data obtained from the body and the generated PPG data, and confirmed that the proposed method can generate stable PPG data. On the other hand, when the waveforms were compared, the generated PPG wave shape differed greatly from the real PPG wave shape, indicating that the software could calculate the heart rate, SDNN, RR interval, and LF/HF ratio regardless of the waveforms. From this, it is clear that calculating the heart rate, SDNN, RR interval, and LF/HF ratio without verifying the waveform is vulnerable to being attacked by fake PPG data.

CCS CONCEPTS

• **Computer systems organization** → **Embedded systems**; *Redundancy*; Robotics; • **Networks** → Network reliability.

KEYWORDS

datasets, neural networks, gaze detection, text tagging

ACM Reference Format:
Atsuhiro Fujii, Kazuya Murao, and Naoji Matsuhisa. 2018. Pulse Wave Generation Method for PPG by using Display. In *Woodstock '18: ACM Symposium on Neural Gaze Detection, June 03–05, 2018, Woodstock, NY*. ACM, New York, NY, USA, 12 pages. https://doi.org/10.1145/1122445.1122456

1 INTRODUCTION

With the growing awareness of health management, wearable devices that record biometric information have become widely used. The biometric information to be recorded includes a variety of data such as activity, respiratory, body temperature, cardiac potential, blood pressure, gaze, pulse wave, and heart rate. The pulse sensor used to acquire these latter two (pulse wave and heart rate) irradiates the skin with LEDs that emit infrared light, red light, or light with a green wavelength around 550 nm. The oxidized hemoglobin in the blood flowing through arteries can absorb these lights. The pulse sensor takes advantage of the fact that the amount of reflected light decreases as the arterial blood flow increases with the timing of the heartbeat, and uses a phototransistor to acquire changes in the amount of reflected light and measure the pulse wave. The pulse wave data is numerical data of the change of the reflected light, and the heart rate is measured by detecting the peaks appearing in the pulse wave data. This type of pulse wave measurement technique is called photoplethysmography (PPG) [1]. PPG sensors today use the same principle as the device introduced by Hertzman [17, 18], but in a smaller size using modern equipment. Many commercially available wearable devices (e.g., smartwatches) are equipped with a PPG sensor as a pulse sensor.

We speculate that it may be possible to measure an arbitrary pulse wave by giving a change of light to the PPG sensor. In this paper, we propose disp2ppg, a method that enables the PPG sensor to acquire pulse data using a display. Paul et al. [38] developed a hardware PPG simulator using an LED array to generate PPG signals,

Woodstock '18, June 03–05, 2018, Woodstock, NY

ACM ISBN 978-1-4503-XXXX-X/18/06…$15.00
https://doi.org/10.1145/1122445.1122456

which was designed to simplify the data collection for photoplethysmography imaging (PPGI). Our disp2ppg method differs in that it aims to use a small device to input data to a PPG sensor equipped on a wearable device. Specifically, it utilizes a smartwatch to measure an arbitrary heart rate. We set two objectives for disp2ppg: PPG transfer and fake PPG.

In terms of PPG transfer, artificial bodies such as prosthetic hands, robotic arms, and telepresence robots do not have any blood flow, which means it is not possible to measure the biometric data even if a smartwatch is worn on the wrist. While smartwatch functions such as calling, messaging, clocking, and payment, as well as sensors such as accelerometers and GPS, can be used in artificial bodies the same as in the living body, pulse data cannot be measured. When a smartwatch is attached to other body parts where blood flow exists (e.g., the ankle) in order to measure pulse data, the usability of other functions (e.g., messaging) is reduced. Other possible methods for PPG transfer include attaching an additional PPG sensor to other body parts where blood flow exists and inputting PPG data wirelessly to the smartwatch, or detecting PPG data (or heart rate data) from sensors other than the PPG [4, 5, 11, 16, 26]. However, since most of the publicly available applications that use PPG data read the values from PPG sensors equipped on the device, PPG data collected by these methods may not be usable for many applications. With the proposed method, even when a smartwatch is attached to an artificial body, it can read the person's pulse data by changing the light of the display under its PPG sensor in accordance with the pulse data measured at the junction of the living body and the prosthetic hand. It is thus possible to use the normal functions of the smartwatch since it is not modified and only the display is mounted on the artificial body. Users can compare various items such as the design, function, and weight of commercial smartwatches and use the model of their choice. In addition, the PPG sensor on the smartwatch acquires the data, without modifying the smartwatch, thus allowing the user to use common applications. When applied to a remote robot avatar, the operator's biometric data can be measured on the avatar's body.

As for fake PPG, if the PPG sensor measures an arbitrary heart rate by the proposed method, it might be possible for a malicious user to falsify the heart rate and pretend to be exercising or continuing to rest. If a device that utilizes the proposed method becomes widely feasible and has a significant social impact, it will be necessary to discuss the use of the current PPG sensor from the viewpoint of its vulnerability.

In the following sections, we introduce related works in Section 2 and explain the details of the proposed method in Section 3. Section 4 discusses the evaluation of the proposed method, Section 5 describes limitations of the proposed method, and finally Section 6 concludes the paper.

2 RELATED WORK

In this section, we introduce research on sensing with wearable devices, the use of smart watches, and the use of pulse data.

2.1 Sensing with wearable devices

Ham et al. [12] have proposed a wristband-type device as an input device for smart glasses. This device is equipped with a touch panel and an inertial measurement unit, and can be operated by touch or a motion such as a twist of the wrist. Since the device can be used by wearing it on the wrist, the user's movement is not restricted and has a high degree of freedom. A touch panel was used for pointing to improve the stability of the input. Hernandez et al. [15] propose a method for recognizing pulse rate and respiration rate from data obtained from the accelerometer, gyroscope, and camera built into Google Glass, a head-worn wearable device. Nishajith et al. [36] designed and implemented Smart Cap as a wearable device to assist the visually impaired with situational awareness. The device consists of a Raspberry Pi 3, a Raspberry Pi NoIR Camera V2, an earphone, and a power supply. The Raspberry Pi NoIR (No Infrared) Camera V2 is an infrared camera module for the Raspberry Pi. The object detected in the image obtained by this infrared camera is described by voice through an earphone. Bello et al. [3] proposed a wearable system that detects body postures and gestures without the need for sensors to be firmly fixed to the body or integrated into a tight-fitting garment. They implemented a prototype "MoCaBlazer" using a standard men's blazer, and conducted evaluation experiments with 14 subjects. For the recognition of 20 actions, the system achieved average recognition accuracy results of 97.18% for leave one recording out and 86.25% for user independent recognition. These are all researches on wearable devices that are worn on body parts, and researches using devices of various shapes have been conducted.

Vargas et al. [50] developed an open-source EEG sensing module with the state-of-the-art analog front-end that is pin/protocol-compatible with popular ecosystems in the wearable and DIY community, with the aim of facilitating broad use of EEG sensing in multi-modal smart garments. They conducted the evaluation experiment using a proof of concept application of the system in a normal baseball cap, and concluded that the system achieved similar levels of recognition as other neuroscience studies with dedicated instruments. Röddiger et al. [41] conducted a study with seven different market-available earables targeted at daytime usage worn by 14 participants each to investigate the comfort and wearability of the earables during sleep. The results showed that devices which occupy more space of the outer ear canal with rigid parts are less desirable. Vekemans et al. [51] implemented "MOTUS", a prototype watchback tactile display that conveys emotions, to explore the potential of emotion expression by displaying tactile texture patterns on the wrist. A preliminary guessability study with the prototype showed agreement between texture patterns and the users' interpretation of emotions. Zhou et al. [55] developed "CoRSA", a lightweight system that enables existing sports apparel with cardiorespiratory monitoring capabilities with system-inpackage (SiP) and system-on-chip (SoC) sensors, which are popular in the wearable computing community. Other studies using ring [10, 25, 35, 40], belt [33, 34, 39, 43], and mask [7, 8, 19, 27] wearable devices also exist.

There are various body parts where wearable devices are worn. Vahdatpour et al. [49] had 25 subjects wear accelerometers at 10 locations on the forearm, upper arm, head, thigh, shin, and waist, and collected acceleration data during daily activities. From the collected data, the SVM (Support Vector Machine) was used to estimate the attachment site with an average accuracy of 89%. Sztyler et al. [46] attached accelerometers to seven locations on the head,

chest, left upper arm, left wrist, waist, left pocket of pants, and left ankle of 15 subjects and collected acceleration data during various physical activities. From the collected data, the wearing site was estimated using Random Forest, and an average accuracy of 89% was achieved. Kunze et al. [28] attached accelerometers to four locations on the wrist, the right side of the head above the eyes, the left trouser's pocket, and the left breast pocket of six subjects and collected data during walking movements. From the collected data, the attachment site was estimated using the C4.5 classifier. We have proposed a method to estimate the body part where the wearer is wearing a wearable device without having the wearer perform a specific action, using ECG and pulse data, which are biometric information that can be acquired by the wearable device [54].

As described above, wearable devices have been proposed in various shapes. Because of the wide range of wearing sites, research using wearable devices has been actively conducted.

2.2 Studies using Smartwatches

Among wearable devices, smartwatches have been commercially available for a long time, and many researches have been conducted. Spinsante et al. [44] focused on the heart rate obtained from a smartwatch during low-intensity physical activity and measured its accuracy. Sen et al. [42] propose a method to record eating behavior, such as whether the user ate with hands, chopsticks, or a spoon, using data obtained from the accelerometer and gyroscope of a smartwatch. By capturing food images with the camera built into the smartwatch and performing image identification, the contents of the meal are also recorded. Johnston et al. [22] focused on the fact that smartwatches are always worn at the same place and in the same direction, and proposed a method for biometric authentication based on gait using data obtained from the accelerometer and gyroscope of the smartwatch. In general, smartphones are often carried in a trouser pocket or handbag. Compared to these locations, activity information tends to appear more on the wrist where the smartwatch is worn. Weiss et al. [53] showed that a smartwatch can identify actions more effectively than a smartphone in hand-based physical behaviors such as eating. For the behavior "drinking", the smartwatch was able to identify the behavior with 93.3% accuracy, while the smartphone could only achieve 77.3% accuracy. Iakovakis et al. [20] are conducting a study aimed at predicting the Blood Pressure (BP) drop caused by postural changes using a smart watch. Orthostatic hypotension (OH) has been shown to cause dizziness and fainting, and is a risk factor for falls in the young as well as the elderly. Therefore, they propose a mathematical prediction model which can reduce the risk of fall due to OH by sensing heart rate variability. Mauldin et al. [32] proposed an Android application "SmartFall" that detects falls using acceleration data obtained from a commercially available smartwatch. The smartwatch is paired with a smartphone that runs SmartFall. SmartFall communicates with a cloud server to perform the calculations necessary to predict falls in real time, while maintaining data privacy. Ciabattoni et al. [6] have proposed a method for detecting mental stress during various cognitive tasks in real time. Galvanic Skin Response (GSR), RR Interval and Body Temperature (BT) acquired by a commercial smartwatch are used to classify stress. Sun et al. [45] present "SleepMonitor", a smartwatch based system for monitoring the respiratory rate and body position. The system uses accelerometer data collected on the wrist to estimate respiratory rate. The results of the evaluation experiments showed that the system can monitor respiratory rate and body position during sleep with high accuracy under various conditions.

On an artificial body, wearable devices can not collect biometric information and thus we may not be able to use these methods. Methods using sensors such as accelerometers and GPS are applicable, but methods using biometric data are not. We try to make these applications available to artificial bodies as well as to living bodies by inputting data to biometric sensors of wearable devices.

2.3 Studies using Pulse Data

Havriushenko et al. [14] have proposed a method for estimating respiratory rate from pulse wave data using neural networks. To measure respiratory rate, thermal sensor placed in nasal channels or elastic chest belt are often used. However, these devices may interfere with sleep. A method of measuring respiratory rate using pulse wave data can be implemented in a wearable device. As a result of the evaluation, the proposed model provides an average respiratory rate estimation error lower than 2.2 breaths per minute. Jarchi et al. [21] proposed a method that relies on a nonlinear time-frequency representation, termed the wavelet synchrosqueezed transform (WSST) to estimate instantaneous respiratory rate (IRR) from body-worn PPG sensors. Han et al. [13] proposed a method for detecting premature atrial contraction (PAC) and premature ventricular contraction (PVC) using PPG data acquired from a smartwatch. Wang et al. [52] developed a system for identifying excess alcohol consumption based on the support vector machine (SVM) algorithm using electrocardiogram (ECG) and PPG monitoring. Longmore et al. [31] conducted a study aimed at identifying a single location on the human anatomy whereby a single PPG sensor could simultaneously measure heart rate (HR), blood oxygen saturation (SpO2), and respiration rate (RR), at rest and while walking. We proposed a method to recognize the muscle-activity state of the arm and a method to estimate sEMG using PPG data [37]. The results of the evaluation experiment with five participants showed that three types of muscle activity were recognized with over 75% accuracy, and sEMG was estimated with an error of approximately 20%.

Goshvarpour et al. [9] have proposed a method for classifying emotional responses by means of a simple dynamic signal processing technique and fusion frameworks. The authors recorded the electrocardiogram and finger pulse activity of 35 participants during rest condition and when subjects were listening to music intended to stimulate certain emotions. After using poincare plots, the SVM was used to classify them into four emotions: happiness, sadness, peacefulness, and fear. Kajiwara et al. [23] focus on the fact that many logistics companies adopt a manual order picking system, and that emotions and engagement affect work efficiency and human errors, and propose a method for predicting emotions and engagement during work with high exercise intensity based on behavior and pulse waves acquired by wearable devices. Pulse wave, eye movements, and movements are input to deep neural networks to estimate emotion and engagement. The results of verification experiments showed that emotion and engagement during order

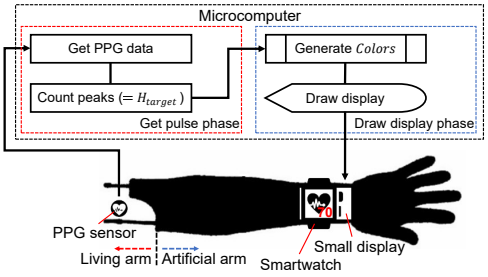

Figure 1: Process flow of proposed method.

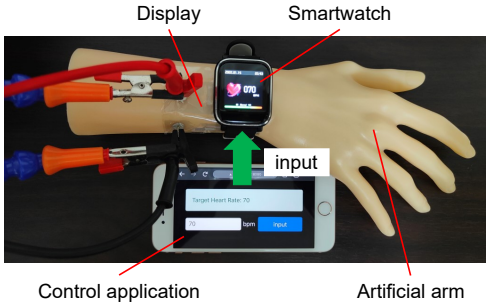

Figure 2: A system in which the target heart rate is manually set from the browser application and the heart rate is input to the smartwatch on the artificial hand.

picking can be predicted from the behavior of the worker with an accuracy of error rate of 0.12 or less. Lee et al. [30] have conducted research on improving the speed of emotion recognition using PPG signal. A two-dimensional emotion model based on valence and arousal is adopted, and one-dimensional convolutional neural network (1D CNN) is used to recognize emotion from 1.1 second PPG signal. They tested the 1D CNN as a binary classification (high or low valence and arousal) using the dataset for emotion analysis using physiological (DEAP) signals, and achieved recognition accuracy of 75.3% for valence and 76.2% for arousal. Udovičić et al. [48] conducted a study on emotion recognition using only galvanic skin response (GSR) and PPG signals because of its suitability for implementation on a simple wearable device that can collect signals from a person without compromising comfort and privacy. There have been many other studies on the use of PPG data for emotion recognition [2, 29, 47].

Pulse data is one of the most important biological information, as it can detect abnormalities in the body and recognize emotions. Most of the pulse sensors in commercially available wearable devices use photoplethysmogram. Therefore, when a wearable device is worn on an artificial body where blood flow does not exist, pulse data cannot be acquired. We focus on pulse data among biometric data, and propose a method to allow a wearable device to measure pulse data similar to that of a living body even on an artificial body.

3 PROPOSED METHOD

This section explains the details of the proposed method.

3.1 Overview

In our proposed method, when a user sets an arbitrary heart rate, the display lights, and a smartwatch worn on the display measures the specified heart rate. The flow of the proposed method is shown in **Figure 1**. First, the real (target) heart rate of the user is obtained with a PPG sensor that is separate from the smartwatch. The proposed method changes the brightness of the display connected to a microcomputer in accordance with the target heart rate. Then, the smartwatch worn over the display measures the heart rate that is the same as the target heart rate.

3.2 Target Heart Rate Calculation

The target heart rate that the proposed method lets the smartwatch measure is the wearer's heart rate obtained using another PPG sensor. Its value can be specified in real time. Let H_{target} be the target heart rate. H_{target} can also be given manually if the user wants the smartwatch to measure a specific heart rate. **Figure 2** shows a system in which the target heart rate is manually set from the browser application and the heart rate is input to the smartwatch on the artificial hand.

3.3 Display Control

The brightness of the display is controlled so that the heart rate measured by the smartwatch becomes H_{target}. An array $Colors$ that holds the brightness of the display to let the smartwatch detect a single pulse is prepared in advance.

The PPG sensors irradiate infrared, red, or green LEDs onto the skin and measure the pulse data from the changes in light reflected through the blood vessels. Because blood flow increases with the timing of the pulse, more light is absorbed by the blood vessels, and the reflected light is dimmer. Since black absorbs more light than white, the more the display is rendered black, the darker the light emitted from the smartwatch worn on the display and reflected through the display.

The proposed method draws the values of $Colors$ on the display one by one for each T[s]. We set the drawing interval T[s] for each value of $Colors$ as follows, so that $Colors$ is played H_{target} times in one minute.

$$T = 60/\{len(Colors) * H_{target}\} \quad (1)$$

$len(Colors)$ is the data length of $Colors$.

3.4 Pulse Data Measurement

In the proposed method, a smartwatch is worn over a blinking display and pulse data is measured. Pulse data measured from a PPG sensor equipped on a smartwatch can be used in various applications. However, the performance of the PPG sensor and the algorithm for measuring the pulse data will vary depending on the model of the smartwatch, and are not disclosed to the public. For this reason, we set the target heart rate manually in our evaluation experiment. We then observe the error between the target heart rate and the heart rate measured by the smartwatch and investigate the effects of the smartwatch model and display.

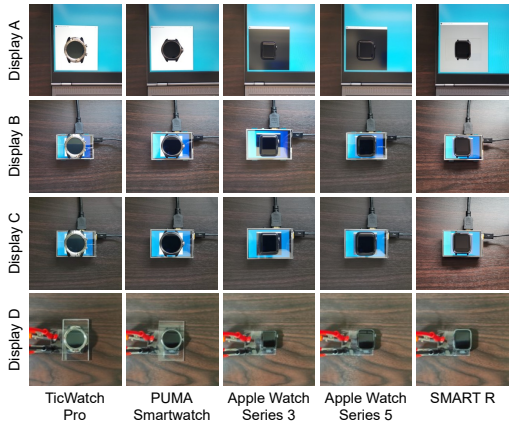

Figure 3: Smartwatches and displays used in the experiment.

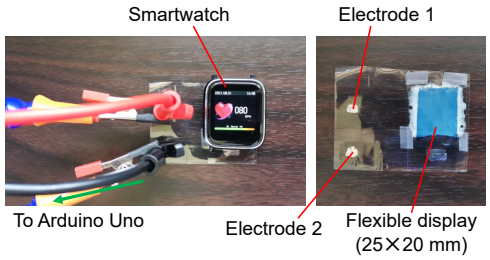

Figure 4: Appearance of the flexible display (Display D).

4 EVALUATION

This section describes the experiments we conducted to evaluate the effectiveness of the proposed method. We measured the heart rate acquired by a smartwatch when an arbitrary target heart rate was given.

4.1 Evaluation Environment

TicWatch Pro WF12106, PUMA Smartwatch, Apple Watch Series 3 and Series 5, and SMART R F-18 were used for the evaluation experiment. For the display, we used the laptop display of Legion 7 15IMH05 by Lenovo (Display A), two small 3.5-inch displays designed for Raspberry Pi by ELECROW and OSOYOO (Displays B and C), and a lightweight flexible display [24] (Display D) we made. The smartwatches and displays A, B, and C are shown in **Figure 3**, and Display D is shown in **Figure 4**.

4.2 *Colors* determination and Display drawing program implementation

Several displays with different connection methods to the computer were used in the evaluation experiments. In this section, we describe the program we implemented to control them.

4.2.1 Displays A, B, C. Since Display A is a laptop display and Displays B and C are displays that can be connected using HDMI, these displays are recognized by the computer as regular displays.

The *Colors* data is represented grayscale, a type of computer color representation that uses 256 levels (0–255) to represent shades of color from black to white. $Colors[i]$ $(i = 0, \ldots, L)$ whose length is L is generated by the following equation.

$$Colors[i] = \min\left(\sin\left(\frac{2\pi i}{L}\right) + 1, 1\right) * SCALE + BASE \quad (2)$$

We determined the values of L, $SCALE$, and $BASE$ heuristically in advance for each display-smartwatch combination.

For example, if $L = 19$, $SCALE = 30$, and $BASE = 225$, then *Colors* was determined to be the following sequence of numbers.

$$Colors = [255, 255, 255, 255, 255, 255, 255, 255, 255, 255,$$
$$250, 240, 232, 227, 225, 225, 229, 236, 245, 255]$$

This *Colors* is plotted in **Figure 5**. The smaller the grayscale, the closer it is to black.

A program to change the brightness and darkness of the display was implemented using Python and Processing. Processing[1] is a programming language based on Java that excels in visual expression, and is used to create electronic art and visual design. Processing receives the target heart rate from the standard input of Python, it uses background method to draw the grayscale as the background color of the window on the display.

4.2.2 Display D. Display D is made of a flexible film that can fit on curved areas like the arm or the back of the smartwatch, but it does not have HDMI. It blinks by switching the potential direction applied to the terminals. The color of the display becomes darker when a higher voltage is applied to electrode 1 and lighter when a higher voltage is applied to electrode 2.

As a result of the heuristic search in the preliminary study, *Colors* was determined to be the following sequence of colors.

$$Colors = [BLACK, WHITE]$$

For *BLACK*, set the voltage of electrode 1 to 2[V] and the voltage of electrode 2 to 0[V], and for *WHITE*, set the voltage of electrode 1 to 0[V] and the voltage of electrode 2 to 2[V]. **Figure 6** shows how the voltage changes when the *Colors* are repeated twice.

We implemented a display drawing program using Arduino Uno R3 microcomputer. This microcomputer can control the output voltage by pulse width modulation (PWM). It receives the target heart rate from the standard input of Python running on a computer connected to it and then changes the voltage to the display.

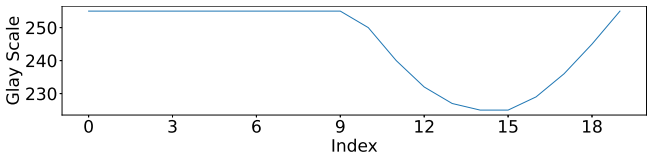

Figure 5: Data of light and dark changes in the display that can make a smartwatch detect a single pulse.

4.3 Data acquisition

A smartwatch is used to measure the heart rate. Smartwatches have different ways of acquiring heart rate depending on the operating

[1]https://processing.org

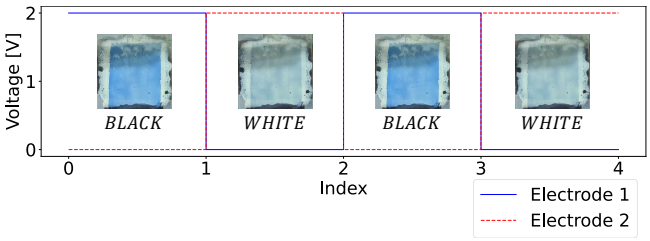

Figure 6: How the voltage changes when the *Colors* are repeated twice.

system they have installed. In this subsection, we describe the methods of obtaining the heart rate for several OSs.

4.3.1 Wear OS by Google. TicWatch Pro WF12106 and PUMA Smartwatch were used in the evaluation experiment. These are both smartwatches run using Wear OS by Google[2], which is an operating system designed for smartwatches based on Google's Android. We implemented the application using Android Studio[3]. The implemented application is shown in **Figure 7**. When we start the application, the screen shown in (1) will be displayed. The acquisition of the sensor value starts automatically, and when there is a change in the value, the sensor value is displayed as shown in (2). "Heart" indicates the value of the heart rate sensor, and "Pulse" indicates the value of the PPG sensor. If we want to record the data, we press the "RECORD" button. Then, the 60-second calibration will start as shown in (3). This calibration waits for the value variation to stabilize. We will adjust the wearing position of the smartwatch during this time. When the 60-second calibration is completed, the sensor data is acquired for 60 seconds as shown in (4) and stored in a variable. At the end of the sensor data acquisition time, the data stored in the variable will be saved in the smartwatch storage in csv format, and a message indicating the completion of data acquisition will be displayed as shown in (5). Sensor number 21 is used to acquire the heart rate data. The rate of events "SENSOR_DELAY_UI" is used to set a sampling rate suitable for the implementation of the user interface[4].

Data acquisition is started by placing the smartwatch on the display, entering the target heart rate into the standard input of the display drawing program, and pressing the "RECORD" button of the smartwatch application. After 120 seconds, including the 60-second calibration, the data acquisition is completed.

The sampling rate for heart rate data acquisition is approximately 1 Hz. In the evaluation experiment, the time average of the 60 seconds of data, excluding the 60 seconds of calibration, was calculated and the result was obtained as one heart rate, as shown in the top of **Figure 8**.

4.3.2 watchOS. Apple Watch Series 3 and Series 5 were used in the experiment. Apple Watch comes standard with the Heart Rate app that measures heart rate[5]. The collected heart rate data can be

[2]https://wearos.google.com
[3]https://developer.android.com/studio
[4]https://developer.android.com/reference/android/hardware/SensorManager
[5]https://support.apple.com/en-us/HT204666

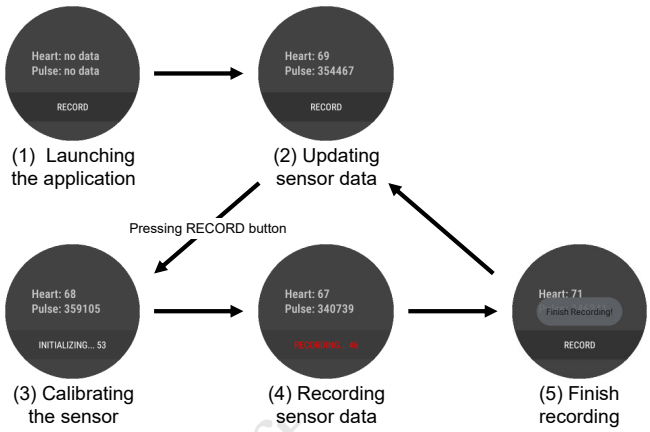

Figure 7: Details of the implemented application.

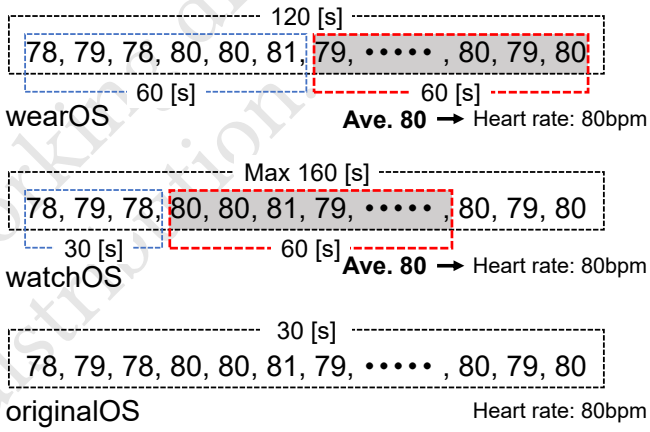

Figure 8: Calculation of heart rate for evaluation experiments with the smartwatches.

output as numerical data in XML format using the iPhone "Health" application paired with Apple Watch[6].

Data acquisition is started by placing the smartwatch on the display, entering the target heart rate into the standard input of the display drawing program, and launching the Heart Rate app. After a while, the Apple Watch display automatically turns off, and the heart rate acquisition is completed. The data acquisition time was not configurable, but the maximum time was approximately 160 seconds.

The sampling rate are not disclosed, and the number of data acquired in a single data acquisition process varies. In the evaluation experiment, as shown in the middle of **Figure 8**, the first 30 seconds of data was excluded as calibration time, and the time average of the data for the following 60 seconds was calculated as the result of one heart rate. However, if there were no data acquired after the calibration time, the last data acquired was used as the resulting heart rate.

[6]https://support.apple.com/guide/iphone/share-health-and-fitness-data-iph27f6325b2/ios

4.3.3 Original OS. The SMART R F-18 used in the experiment is equipped with a proprietary operating system developed by the manufacturer. Heart rate data collected by this smartwatch can be viewed on the "WearHealth" application developed for Android and iPhone[7][8].

Data acquisition is started by placing the smartwatch on the display, entering the target heart rate into the standard input of the display drawing program, and operating the "WearHealth" application on the smartphone. After 30 seconds, the data acquisition was finished, and the resulting one heart rate was displayed on the application.

The sampling rate and the algorithm to determine the resulting heart rate are not disclosed. In the evaluation experiment, the one heart rate of the result displayed on the application, as shown in the bottom of **Figure 8**, was recorded manually.

4.4 Results and Discussion

To obtain the correct heart rate, an acrylic plate of some thickness was placed between the display and a smartwatch in some display-smartwatch combinations. The display-smartwatch combinations and the thickness of the placed acrylic plate are shown in **Table 1**. A blank cell indicates that the acrylic plate was not placed.

The smartwatches were placed on the display and the target heart rate was input to the display drawing program. The error of the measured heart rate was calculated by subtracting the measurement from the target, and that was taken as the result. The target heart rate was tested at intervals of 5 from 60 to 100 beats per minute (bpm), which is a resting heart rate range for adults[9]. The results of the evaluation experiment are shown in **Table 2**, where the results are the average of three sets. Zero means that the heart rate was the same as the target heart rate, and minus means that the heart rate was smaller. *NaN* indicates that the heart rate measurement has failed.

In addition, we conducted evaluation experiments using Display D with target heart rates set at 40–55 (heart rate during sleep) and 105–200 (heart rate during exercise). The results are shown in **Table 3**.

4.4.1 WearOS Smartwatch. The results showed that the heart rate could be input to the smartwatch within an error of less than 3 bpm. In both wearOS smartwatch results, the average error was smaller for Displays A, B, C, and D, in that order. This suggests that differences in performance, such as display brightness and refresh rate, may affect the generated heart rate.

Even when the characteristic heart rate was set as the target heart rate, the heart rate could be input to the smartwatch with a small error.

4.4.2 WatchOS Smartwatch. The results showed that using Display C enabled the heart rate to be input to the Apple Watch within an error of −1.1 to 0.1 bpm. On the other hand, when using Display A or B, it was not possible to obtain the correct heart rate under some conditions. The correct heart rate was not obtained even once, when the target heart rate was set to 60 with the combination of Apple Watch Series 5 and Display A.

For the characteristic target heart rates, correct values were obtained for some target heart rates when using Apple Watch Series 5. When the target heart rate was set above 100, the obtained heart rate was very small compared to the target heart rate. It is possible that the large target heart rate was recognized by the Apple Watch algorithm as an incorrect heart rate and was calibrated to the resting heart rate.

The combination of Apple Watch Series 3 and Display D failed to measure the heart rate regardless of the target heart rate. Since the PPG sensor uses a photoreflector, they are easily affected by light, and depending on the condition of the position where the device is placed, the pulse data cannot be acquired correctly. Whether or not the generated pulse wave can be recognized by the smartwatch is thought to depend on the shape of the PPG sensor part of the device. The acrylic plate we prepared in this paper could not support Apple Watch Series 3, but there is a possibility that the pulse data can be input by placing a material of other materials and thickness.

4.4.3 OriginalOS Smartwatch. The results showed that the heart rate could be input to the smartwatch within an error of almost less than 3 bpm. Especially for Display D, the heart rate could be input to the smartwatch within an error of less than 1 bpm.

When the target heart rate was a characteristic heart rate, the heart rate could be input into the smartwatch with a very small error in many cases, but for target heart rates below 50, the heart rate could not be input correctly. This is thought to be due to the performance limitation of the PPG sensor in the smartwatch.

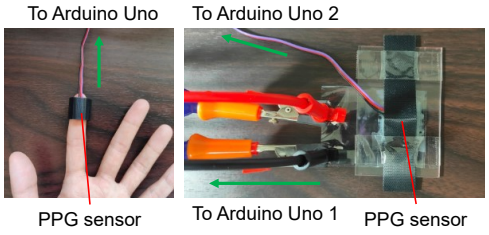

Figure 9: The environment during raw pulse data acquisition.

5 LIMITATIONS

From the results in Section 4, the heart rate could be input into the smartwatch with small errors. This section discusses the limitations of the proposed method in terms of other pulse wave related indices and pulse wave waveform.

In order to compare, the real raw PPG data of the author's left index finger and the raw PPG data generated by Display D with 2-mm acrylic plate were acquired. The environment during raw pulse data acquisition is shown in **Figure 9**. Numerical pulse data was collected at a sampling rate of 106 Hz for 60 seconds using Arduino Uno R3 and a PPG sensor manufactured by pulsesensor.com. The Arduino used here is a different one from the one used to control the display.

[7]https://play.google.com/store/apps/details?id=com.zjw.wearhealth
[8]https://apps.apple.com/us/app/wearhealth/id1265052549
[9]https://www.heart.org/en/healthy-living/fitness/fitness-basics/target-heart-rates

Table 1: The thickness of the placed acrylic plate.

TicWatch Pro				PUMA				Series 3				Series 5				SMART R			
A	B	C	D	A	B	C	D	A	B	C	D	A	B	C	D	A	B	C	D
–	2-mm	–	5-mm	–	–	–	2-mm	–	–	–	–	–	2-mm	–	–	2-mm	–	–	–

Table 2: Error of resting heart rate obtained by TicWatch Pro, PUMA Smartwatch, Apple Watch Series 3, Apple Watch Series 5, and SMART R. (Display A: Lenovo Legion 7, B: 3.5-inch ELECROW, C: 3.5-inch OSOYOO, D: flexible display)

	TicWatch Pro				PUMA			
H_{target}	A	B	C	D	A	B	C	D
60	−1.7	−1.4	−1.4	−2.0	−1.7	−1.4	−1.4	−0.8
65	−1.8	−1.4	−1.3	−2.5	−1.8	−1.4	−1.3	−1.8
70	−1.8	−2.1	−1.2	−0.4	−1.8	−2.1	−1.2	−0.9
75	−2.2	−1.6	−1.5	−0.1	−2.2	−1.6	−1.5	−1.2
80	−2.0	−1.5	−1.1	0.6	−2.0	−1.5	−1.1	0.0
85	−1.8	−1.5	−1.6	0.5	−1.8	−1.5	−1.6	0.3
90	−2.0	−1.7	−1.0	−0.4	−2.0	−1.7	−1.0	−0.5
95	−2.0	−1.2	−1.1	0.0	−2.0	−1.2	−1.1	−1.2
100	−1.9	−1.5	−1.4	−1.0	−1.9	−1.5	−1.4	−1.2
Average	−1.9	−1.5	−1.3	−0.6	−1.9	−1.5	−1.3	−0.8

	Series 3				Series 5				SMART R			
H_{target}	A	B	C	D	A	B	C	D	A	B	C	D
60	0.4	1.0	−0.2	NaN	58.2	0.1	−0.1	0.0	−1.7	−1.0	−1.7	−0.7
65	0.6	0.1	−0.1	NaN	16.1	−0.4	0.1	0.0	−1.7	−1.0	−0.7	−0.7
70	0.1	2.0	0.0	NaN	1.6	2.4	0.1	0.0	−1.0	−1.3	−1.3	−0.7
75	0.0	2.8	−0.6	NaN	0.8	0.1	−0.2	−0.1	−2.0	−2.3	−2.0	−0.7
80	−0.5	1.0	−0.5	NaN	1.2	0.9	−0.4	−0.5	−2.0	−2.0	−1.0	−1.0
85	−5.4	−0.7	−0.6	NaN	−0.6	−1.0	−0.9	0.0	−2.0	−2.0	−1.7	−0.7
90	−0.6	−1.3	−0.6	NaN	4.3	−1.0	−0.9	0.0	−3.3	−2.3	−1.7	−1.0
95	−1.5	−0.5	−1.0	NaN	−0.1	−0.3	−1.1	0.0	−2.7	−2.0	−2.0	−0.3
100	−0.7	−1.1	−0.7	NaN	−0.2	−7.3	−0.8	−32.7	−2.7	−2.3	−2.7	−1.0
Average	−0.8	0.4	−0.5	NaN	9.0	−0.7	−0.5	−3.7	−2.1	−1.8	−1.6	−0.7

5.1 Pulse wave status indicators

The raw PPG data obtained was analyzed using Kubios HRV Premium (ver. 3.5.0)[10], a full featured heart rate variability (HRV) analysis software for scientific research and professional use. The analysis was performed without changing the settings from the defaults at the time of data import. **Table 4** shows the results of analysis of the real PPG data, and **Table 5** shows the results of analysis of the generated PPG data. RR Time Series data are plotted in **Figure 10**. The target heart rate at the time of pulse wave generation was set to 68 bpm, which is the same as the mean heart rate of the real pulse wave obtained from the finger. From the results, it can be seen that the generated pulse wave is 68 for both Min HR and Max HR, and the target heart rate can be input to the PPG sensor in a stable manner as in the evaluation experiment in section 4. Mean RR was close and normal between the real and generated pulse waves, indicating that the generated pulse wave could be recognized as a correctly pulse wave waveform. SDNN of the generated pulse wave showed a very small value. SDNN is the standard deviation of RR interval, and since the mechanically generated pulse wave was a stable waveform, no variation in RR interval occurred and SDNN may have been small. The fact that there is no variation in RR intervals can be seen in **Figure 10**. HF, also known as respiratory sinus arrhythmia (RSA), is the variation of RR interval with respiration. When HF is high, it indicates that the parasympathetic nervous system is dominant and respiratory cycle is regular. From Power (%) and LF/HF ratio of the generated pulse wave, it can be seen that HF is very large and the mechanically generated pulse wave is a stable waveform without any turbulence.

5.2 Pulse wave waveform

The first 10 seconds of the obtained raw PPG data are plotted in **Figure 11**. The real pulse wave varies in amplitude and is not stable, but the generated pulse wave is a stable waveform. However, the generated pulse waveform does not resemble the real pulse waveform, and the similarity between the waveforms is low. Even if the waveform is an irregular, it is recognized as a pulse wave by the smartwatch and analysis software, and indicators such as heart rate are calculated. Therefore, since the calculation of the pulse wave state indicators depends on the algorithm of each product, it

[10] https://www.kubios.com/hrv-premium

Table 3: Error of characteristic heart rate obtained by TicWatch Pro, PUMA Smartwatch, Apple Watch Series 3, Apple Watch Series 5, and SMART R. (Display D: flexible display)

H_{target}	TicWatch Pro D	PUMA D	Series 3 D	Series 5 D	SMART R D
40	0.0	0.0	NaN	3.1	23.7
45	−1.2	−1.0	NaN	0.1	31.7
50	−1.7	−0.8	NaN	0.0	0.3
55	−0.7	−0.7	NaN	0.0	0.0
⋮	⋮	⋮	⋮	⋮	⋮
105	−0.2	0.0	NaN	−34.3	0.0
110	−0.2	0.0	NaN	−0.2	−0.3
115	−0.2	0.3	NaN	−39.3	−0.3
120	−0.3	−0.7	NaN	−41.5	−0.7
125	−0.8	0.0	NaN	−0.7	−0.3
130	0.9	0.3	NaN	−41.9	0.0
135	0.0	−0.8	NaN	−41.7	−0.3
140	0.2	−0.3	NaN	−70.7	0.0
145	0.7	−0.2	NaN	−40.2	0.3
150	−0.1	−0.3	NaN	−0.6	−0.3
155	0.5	0.0	NaN	0.1	0.0
160	0.6	0.0	NaN	0.0	−0.3
165	1.7	1.3	NaN	0.0	0.7
170	0.0	0.7	NaN	−94.4	0.0
175	0.3	0.0	NaN	−50.6	−0.7
180	0.3	0.6	NaN	−63.0	0.0
185	1.0	−0.4	NaN	−0.3	0.3
190	1.4	−0.2	NaN	−86.8	0.3
195	0.3	1.7	NaN	−83.4	0.3
200	0.6	0.0	NaN	−103.0	0.0

Table 4: Status evaluation index report of the real PPG data.

Time-Domain Results

Variable	Units	Value
Mean RR	(ms)	887
Mean HR	(bpm)	68
Min HR	(bpm)	63
Max HR	(bpm)	74
SDNN	(ms)	37.5
RMSSD	(ms)	49.4
NN50	(beats)	20
pNN50	(%)	33.90
RR triangular index		7.50
TINN	(ms)	149.0
Stress Index (SI)		12.8
DC	(ms)	26.6
DCmod	(ms)	51.4

Frequency-Domain Results (FFT spectrum)

Variable	Units	VLF	LF	HF
Frequency band	(Hz)	0.00–0.04	0.04–0.15	0.15–0.40
Peak frequency	(Hz)	0.040	0.113	0.350
Power	(ms^2)	113	800	657
Power	(log)	4.726	6.684	6.488
Power	(%)	7.17	50.84	41.79
Power	(n.u.)		54.77	45.02

Total power	(ms^2)	1573		
Total power	(log)	7.361		
LF/HF ratio		1.216		
RESP	(Hz)	–		

is necessary to check the raw data waveform in order to verify that it is genuine PPG data. Since the PPG sensor use a photoreflector to read the amount of change in light, they are susceptible to the effects of external light due to changes in the mounting position. The proposed method determined the optimal *Colors* heuristically, but it is difficult to deal with the noise. To deal with this problem and make the generated pulse waveform resemble the real pulse waveform, it is necessary to automate the *Colors* determination.

6 CONCLUSION

In this paper, we proposed a method that enables a PPG sensor to measure arbitrary pulse wave using display. We implemented display drawing programs and conducted evaluation experiments using five kinds of smartwatches and four kinds of displays to determine the effectiveness of the proposed method. The results showed that the error between the target heart rate and the heart rate acquired by the smartwatch was within 3 beats per minute in

Table 5: Status evaluation index report of the generated PPG data.

Time-Domain Results

Variable	Units	Value
Mean RR	(ms)	883
Mean HR	(bpm)	68
Min HR	(bpm)	68
Max HR	(bpm)	68
SDNN	(ms)	1.9
RMSSD	(ms)	3.1
NN50	(beats)	0
pNN50	(%)	0.00
RR triangular index		NaN
TINN	(ms)	7.0
Stress Index (SI)		81.7
DC	(ms)	1.0
DCmod	(ms)	3.2

Frequency-Domain Results (FFT spectrum)

Variable	Units	VLF	LF	HF
Frequency band	(Hz)	0.00–0.04	0.04–0.15	0.15–0.40
Peak frequency	(Hz)	0.030	0.120	0.287
Power	(ms^2)	0	0	1
Power	(log)	0.000	0.000	0.088
Power	(%)	1.64	25.16	73.00
Power	(n.u.)		25.57	74.22

Total power	(ms^2)	1		
Total power	(log)	0.403		
LF/HF ratio		0.345		
RESP	(Hz)	–		

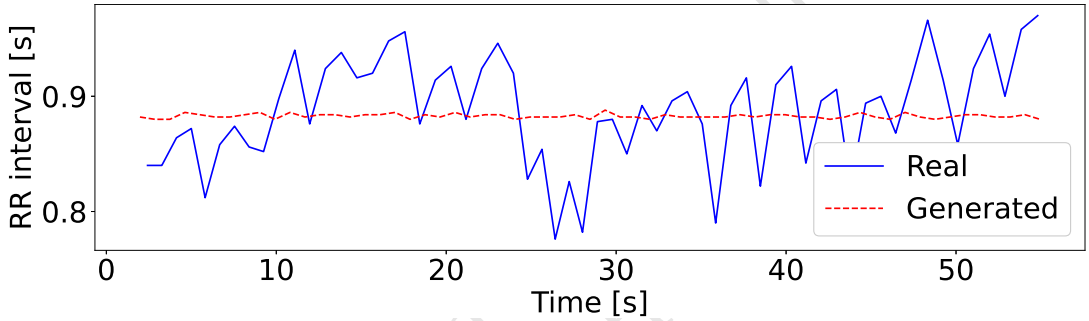

Figure 10: RR Time Series data.

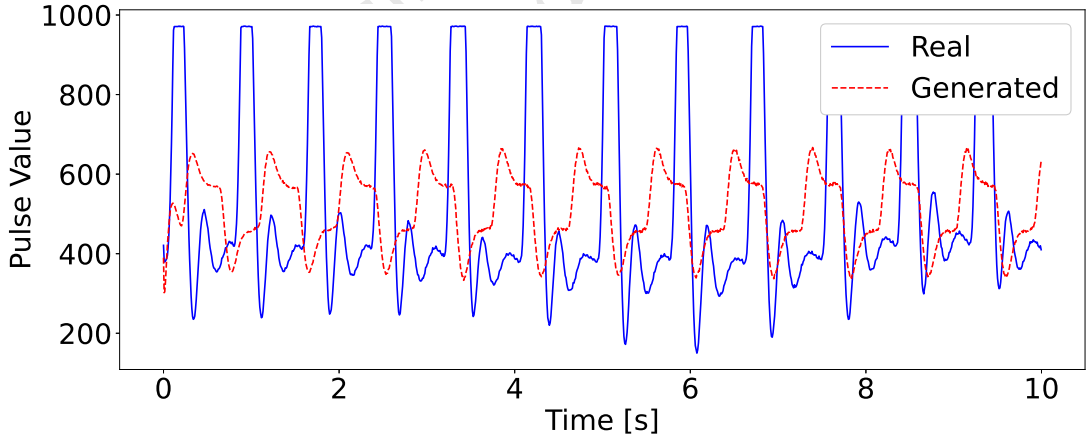

Figure 11: Raw PPG data.

many cases when the target heart rate was set to 60–100. When the target heart rate was set to 40–55 and 105–200, the heart rate could be input to the smartwatch with a small error under some conditions. When the generated PPG data was imported into a heart rate variability (HRV) analysis software, it was recognized as a pulse wave in the same way as real PPG data obtained from a body. We compared the heart rate, SDNN, RR interval, and LF/HF ratio calculated from the real PPG data obtained from the body and the generated PPG data, and confirmed that the proposed method can generate stable PPG data. On the other hand, when the waveforms were compared, the generated PPG wave shape differed greatly from the real PPG wave shape, indicating that the software could calculate the heart rate, SDNN, RR interval, and LF/HF ratio regardless of the waveforms. From this, it is clear that calculating the

heart rate, SDNN, RR interval, and LF/HF ratio without verifying the waveform is vulnerable to being attacked by fake PPG data.

In future work, we will improve the reproducibility of PPG data for use in a real environment and implement a mechanism that enables the wearable device worn on the display to measure the same PPG data by inputting PPG data obtained from a live body part. To achieve this, the system needs to automatically determine the colors to be drawn on the display while calibrating for the environment, so we will build a generative model that can output the color to be drawn by inputting PPG data.

REFERENCES

[1] John Allen. 2007. Photoplethysmography and its application in clinical physiological measurement. *Physiological Measurement* 28, 3 (feb 2007), R1–R39.

[2] Değer Ayata, Yusuf Yaslan, and Mustafa E. Kamasak. 2020. Emotion Recognition from Multimodal Physiological Signals for Emotion Aware Healthcare Systems. *Journal of Medical and Biological Engineering* 40, 2 (01 Apr 2020), 149–157.

[3] Hymalai Bello, Bo Zhou, Sungho Suh, and Paul Lukowicz. 2021. *MoCapaci: Posture and Gesture Detection in Loose Garments Using Textile Cables as Capacitive Antennas.* 78–83.

[4] Gerald Bieber, Marian Haescher, and Matthias Vahl. 2013. Sensor Requirements for Activity Recognition on Smart Watches. In *Proceedings of the 6th International Conference on PErvasive Technologies Related to Assistive Environments (PETRA '13).* Article 67, 6 pages.

[5] Jennifer C.Dela Cruz, Jonathan Ibera, Joshua M. Alcoy, and Cyril Erick R. Tulio. 2021. Deriving Heart Rate and Respiratory Rate from ECG Using Wavelet Transform. In *2021 11th International Conference on Biomedical Engineering and Technology (ICBET '21).* 100–105.

[6] Lucio Ciabattoni, Francesco Ferracuti, Sauro Longhi, Lucia Pepa, Luca Romeo, and Federica Verdini. 2017. Real-time mental stress detection based on smartwatch. In *2017 IEEE International Conference on Consumer Electronics (ICCE).* 110–111.

[7] Hannah Friederike Fischer, Daniela Wittmann, Alejandro Baucells Costa, Bo Zhou, Gesche Joost, and Paul Lukowicz. 2021. *Masquare: A Functional Smart Mask Design for Health Monitoring.* 175–178.

[8] Çağlar Genç, Ashley Colley, Markus Löchtefeld, and Jonna Häkkilä. 2020. Face Mask Design to Mitigate Facial Expression Occlusion. In *Proceedings of the 2020 International Symposium on Wearable Computers (ISWC '20).* 40–44.

[9] Atefeh Goshvarpour, Ataollah Abbasi, and Ateke Goshvarpour. 2017. Fusion of heart rate variability and pulse rate variability for emotion recognition using lagged poincare plots. *Australasian Physical & Engineering Sciences in Medicine* 40, 3 (2017), 617–629.

[10] Jeremy Gummeson, Bodhi Priyantha, and Jie Liu. 2014. An Energy Harvesting Wearable Ring Platform for Gestureinput on Surfaces. In *Proceedings of the 12th Annual International Conference on Mobile Systems, Applications, and Services (MobiSys '14).* 162–175.

[11] Marian Haescher, Denys J.C. Matthies, John Trimpop, and Bodo Urban. 2016. SeismoTracker: Upgrade Any Smart Wearable to Enable a Sensing of Heart Rate, Respiration Rate, and Microvibrations. In *Proceedings of the 2016 CHI Conference Extended Abstracts on Human Factors in Computing Systems (CHI EA '16).* 2209–2216.

[12] Jooyeun Ham, Jonggi Hong, Youngkyoon Jang, Seung Hwan Ko, and Woontack Woo. 2014. Smart Wristband: Touch-and-Motion–Tracking Wearable 3D Input Device for Smart Glasses. In *Distributed, Ambient, and Pervasive Interactions.* 109–118.

[13] Dong Han, Syed Khairul Bashar, Fahimeh Mohagheghian, Eric Ding, Cody Whitcomb, David D. McManus, and Ki H. Chon. 2020. Premature Atrial and Ventricular Contraction Detection using Photoplethysmographic Data from a Smartwatch. *Sensors* 20, 19 (2020), 5683.

[14] Anastasiia Havriushenko, Kostyantyn Slyusarenko, and Illia Fedorin. 2020. Smartwatch based respiratory rate estimation during sleep using CNN/LSTM neural network. In *Proceedings of IEEE 40th International Conference on Electronics and Nanotechnology (ELNANO 2020).* 584–587.

[15] J. Hernandez, Y. Li, J. M. Rehg, and R. W. Picard. 2014. BioGlass: Physiological parameter estimation using a head-mounted wearable device. In *2014 4th International Conference on Wireless Mobile Communication and Healthcare - Transforming Healthcare Through Innovations in Mobile and Wireless Technologies (MOBIHEALTH).* 55–58.

[16] Javier Hernandez, Daniel McDuff, and Rosalind W. Picard. 2015. Biowatch: Estimation of heart and breathing rates from wrist motions. In *Proceedings of 9th International Conference on Pervasive Computing Technologies for Healthcare (PervasiveHealth 2015).* 169–176.

[17] Alrick B. Hertzman. 1938. Comparative Estimation of Blood Supply of Skin Areas from Photoelectrically Recorded Volume Pulse. *Proceedings of the Society for Experimental Biology and Medicine* 38, 4 (1938), 562–564.

[18] Alrick B. Hertzman. 1938. THE BLOOD SUPPLY OF VARIOUS SKIN AREAS AS ESTIMATED BY THE PHOTOELECTRIC PLETHYSMOGRAPH. *American Journal of Physiology-Legacy Content* 124, 2 (1938), 328–340.

[19] Hirotaka Hiraki and Jun Rekimoto. 2021. SilentMask: Mask-Type Silent Speech Interface with Measurement of Mouth Movement. In *Augmented Humans Conference 2021 (AHs'21).* 86–90.

[20] Dimitrios Iakovakis and Leontios Hadjileontiadis. 2016. Standing Hypotension Prediction Based on Smartwatch Heart Rate Variability Data: A Novel Approach. In *Proceedings of the 18th International Conference on Human-Computer Interaction with Mobile Devices and Services Adjunct.* 1109–1112.

[21] Delaram Jarchi, Dario Salvi, Lionel Tarassenko, and David A. Clifton. 2018. Validation of Instantaneous Respiratory Rate Using Reflectance PPG from Different Body Positions. *Sensors* 18, 11 (2018).

[22] Andrew H. Johnston and Gary M. Weiss. 2015. Smartwatch-based biometric gait recognition. In *Proceedings of 2015 IEEE 7th International Conference on Biometrics Theory, Applications and Systems (BTAS).* 1–6.

[23] Yusuke Kajiwara, Toshihiko Shimauchi, and Haruhiko Kimura. 2019. Predicting Emotion and Engagement of Workers in Order Picking Based on Behavior and Pulse Waves Acquired by Wearable Devices. *Sensors* 19, 1 (2019).

[24] Jun Kawahara, Peter Andersson Ersman, Isak Engquist, and Magnus Berggren. 2012. Improving the color switch contrast in PEDOT:PSS-based electrochromic displays. *Organic Electronics* 13, 3 (2012), 469–474.

[25] Wolf Kienzle, Eric Whitmire, Chris Rittaler, and Hrvoje Benko. 2021. *ElectroRing: Subtle Pinch and Touch Detection with a Ring.*

[26] Sanjay Kimbahune, Sujit Shinde, Karan Bhavsar, Avik Ghose, Sundeep Khandelwal, and Arpan Pal. 2021. Heart Rate Monitoring Using Capacitive Touchscreen Sensing. In *Proceedings of the Workshop on Body-Centric Computing Systems (BodySys'21).* 13–17.

[27] Ryoga Kumazaki and Akifumi Inoue. 2019. Development and Evaluation of a Mask-Type Display Transforming the Wearer's Impression. In *Proceedings of the 31st Australian Conference on Human-Computer-Interaction (OZCHI'19).* 568–571.

[28] Kai Kunze, Paul Lukowicz, Holger Junker, and Gerhard Tröster. 2005. Where am I: Recognizing On-body Positions of Wearable Sensors. In *Location- and Context-Awareness.* 264–275.

[29] Min Lee., Ye Cho., Yun Lee., Dong Pae., Myo Lim., and Tae Kang. 2019. PPG and EMG Based Emotion Recognition using Convolutional Neural Network. In *Proceedings of the 16th International Conference on Informatics in Control, Automation and Robotics - Volume 1: ICINCO,.* INSTICC, 595–600.

[30] Min Seop Lee, Yun Kyu Lee, Dong Sung Pae, Myo Taeg Lim, Dong Won Kim, and Tae Koo Kang. 2019. Fast Emotion Recognition Based on Single Pulse PPG Signal with Convolutional Neural Network. *Applied Sciences* 9, 16 (2019).

[31] Sally K. Longmore, Gough Y. Lui, Ganesh Naik, Paul P. Breen, Bin Jalaludin, and Gaetano D. Gargiulo. 2019. A Comparison of Reflective Photoplethysmography for Detection of Heart Rate, Blood Oxygen Saturation, and Respiration Rate at Various Anatomical Locations. *Sensors* 19, 8 (2019).

[32] Taylor R. Mauldin, Marc E. Canby, Vangelis Metsis, Anne H. H. Ngu, and Coralys Cubero Rivera. 2018. SmartFall: A Smartwatch-Based Fall Detection System Using Deep Learning. *Sensors* 18, 10 (2018).

[33] Yugo Nakamura, Yuki Matsuda, Yutaka Arakawa, and Keiichi Yasumoto. 2019. WaistonBelt X: A Belt-Type Wearable Device with Sensing and Intervention Toward Health Behavior Change. *Sensors* 19, 20 (2019).

[34] Hyejeong Nam, Jin-Hyun Kim, and Jee-In Kim. 2016. Smart Belt : A wearable device for managing abdominal obesity. In *2016 International Conference on Big Data and Smart Computing (BigComp).* 430–434.

[35] Shahriar Nirjon, Jeremy Gummeson, Dan Gelb, and Kyu-Han Kim. 2015. TypingRing: A Wearable Ring Platform for Text Input. In *Proceedings of the 13th Annual International Conference on Mobile Systems, Applications, and Services (MobiSys '15).* 227–239.

[36] A. Nishajith, J. Nivedha, S. S. Nair, and J. Mohammed Shaffi. 2018. Smart Cap - Wearable Visual Guidance System for Blind. In *2018 International Conference on Inventive Research in Computing Applications (ICIRCA).* 275–278.

[37] Masahiro Okamoto and Kazuya Murao. 2021. *Estimating Upper Arm SEMG from Wrist PPG.* 147–149.

[38] Michael Paul, Ana Filipa Mota, Christoph Hoog Antink, Vladimir Blazek, and Steffen Leonhardt. 2019. Modeling photoplethysmographic signals in camera-based perfusion measurements: optoelectronic skin phantom. *Biomed. Opt. Express* 9 (2019), 4353–4368.

[39] Emanuele Piuzzi, Stefano Pisa, Erika Pittella, Luca Podestà, and Silvia Sangiovanni. 2020. Wearable Belt With Built-In Textile Electrodes for Cardio—Respiratory Monitoring. *Sensors* 20, 16 (2020).

[40] Gilang Andi Pradana, Adrian David Cheok, Masahiko Inami, Jordan Tewell, and Yongsoon Choi. 2014. Emotional Priming of Mobile Text Messages with Ring-Shaped Wearable Device Using Color Lighting and Tactile Expressions. In *Proceedings of the 5th Augmented Human International Conference (AH '14).* Article 14, 8 pages.

[41] Tobias Röddiger, Christian Dinse, and Michael Beigl. 2021. Wearability and Comfort of Earables During Sleep. In *2021 International Symposium on Wearable*

Computers (Virtual, USA) *(ISWC '21)*. 150–152.
[42] Sougata Sen, Vigneshwaran Subbaraju, Archan Misra, Rajesh Krishna Balan, and Youngki Lee. 2015. The case for smartwatch-based diet monitoring. In *2015 IEEE International Conference on Pervasive Computing and Communication Workshops (PerCom Workshops)*. 585–590.
[43] Wann-Yun Shieh, Tyng-Tyng Guu, and An-Peng Liu. 2013. A portable smart belt design for home-based gait parameter collection. In *2013 International Conference on Computational Problem-Solving (ICCP)*. 16–19.
[44] S. Spinsante, S. Porfiri, and L. Scalise. 2019. Accuracy of Heart Rate Measurements by a Smartwatch in Low Intensity Activities. In *2019 IEEE International Symposium on Medical Measurements and Applications (MeMeA)*. 1–6.
[45] Xiao Sun, Li Qiu, Yibo Wu, Yeming Tang, and Guohong Cao. 2017. SleepMonitor: Monitoring Respiratory Rate and Body Position During Sleep Using Smartwatch. *Proc. ACM Interact. Mob. Wearable Ubiquitous Technol.* 1, 3, Article 104 (sep 2017), 22 pages.
[46] Timo Sztyler, Heiner Stuckenschmidt, and Wolfgang Petrich. 2017. Position-aware activity recognition with wearable devices. *Pervasive and Mobile Computing* 38 (2017), 281 – 295.
[47] Zhongkai Tong, XianXiang Chen, Zhengling He, Kai Tong, Zhen Fang, and Xianlong Wang. 2018. Emotion Recognition Based on Photoplethysmogram and Electroencephalogram. In *2018 IEEE 42nd Annual Computer Software and Applications Conference (COMPSAC)*, Vol. 02. 402–407.
[48] Goran Udovičić, Jurica Đerek, Mladen Russo, and Marjan Sikora. 2017. Wearable Emotion Recognition System Based on GSR and PPG Signals. In *Proceedings of the 2nd International Workshop on Multimedia for Personal Health and Health Care (MMHealth '17)*. 53–59.
[49] A. Vahdatpour, N. Amini, and M. Sarrafzadeh. 2011. On-body device localization for health and medical monitoring applications. In *2011 IEEE International Conference on Pervasive Computing and Communications (PerCom)*. 37–44.
[50] Juan Felipe Vargas, Bo Zhou, Hymalai Bello, and Paul Lukowicz. 2021. Brainwear: Towards Multi-Modal Garment Integrated EEG. In *2021 International Symposium on Wearable Computers (ISWC '21)*. 113–118.
[51] Verindi Vekemans, Ward Leenders, Sijie Zhu, and Rong-Hao Liang. 2021. *MOTUS: Rendering Emotions with a Wrist-Worn Tactile Display.* 159–161.
[52] Wen-Fong Wang, Ching-Yu Yang, and Yan-Fu Wu. 2018. SVM-Based Classification Method to Identify Alcohol Consumption Using ECG and PPG Monitoring. *Personal and Ubiquitous Computing* 22, 2 (Apr 2018), 275–287.
[53] Gary M. Weiss, Jessica L. Timko, Catherine M. Gallagher, Kenichi Yoneda, and Andrew J. Schreiber. 2016. Smartwatch-based activity recognition: A machine learning approach. In *2016 IEEE-EMBS International Conference on Biomedical and Health Informatics (BHI)*. 426–429.
[54] Kazuki Yoshida and Kazuya Murao. 2019. Estimating Load Positions of Wearable Devices Based on Difference in Pulse Wave Arrival Time. In *Proceedings of the 23rd International Symposium on Wearable Computers (ISWC)*. 234–243.
[55] Bo Zhou, Alejandro Baucells Costa, and Paul Lukowicz. 2019. CoRSA: A Cardio-Respiratory Monitor in Sport Activities. In *Proceedings of the 23rd International Symposium on Wearable Computers (ISWC '19)*. 254–256.